Journal of Electrical Engineering & Technology
https://doi.org/10.1007/s42835-024-01893-w

ORIGINAL ARTICLE

Robust Event-triggered Fuzzy Energy-to-peak Disturbance Attenuation for Wheeled Mobile Robots

Sung Chul Jee[1] · Ho Jae Lee[2]

Received: 18 February 2024 / Revised: 5 March 2024 / Accepted: 18 March 2024

Abstract
We explore the robust tracking problem for nonholonomic wheeled mobile robots (WMR) in the presence of uncertainties. The kinematics of the WMR are represented in the Takagi–Sugeno fuzzy form without modeling error. Recognizing the inherent challenge of obtaining a discrete-time model for time-triggered sampled-data controller design, we adopt an event-triggered sampled-data controller. The designed controller guarantees notable $\mathcal{L}_2$–$\mathcal{L}_\infty$ disturbance attenuation performance and robustness against norm-bounded parametric uncertainties, excluding the Zeno phenomenon in the event triggering. Results of the case study about the WMR model demonstrate the efficacy of the proposed methodology.

Keywords Wheeled mobile robot (WMR) · Takagi–Sugeno fuzzy model; event-triggered control · $\mathcal{L}_2$–$\mathcal{L}_\infty$ disturbance attenuation

1 Introduction

The aging of the agroforestry workforce, combined with the ongoing trend of urbanization, prompts significant concerns about a food shortfall soon. Mitigating the resultant workforce imbalance requires the implementation of mechanization in agroforestry processes, with autonomous wheeled mobile robots (WMR) emerging as a promising solution [21]. For example, WMRs can implement changeable transport paths, overcoming the limitations associated with fixed conveyor belts [16]. In this scenario, the primary objective of a WMR, viewed through the lens of control engineering, is cast as a nonlinear tracking control problem.

The authors of [13] developed an adaptive sliding mode control approach for a WMF with uncertainties. In [14], they further deliberated the (electric) actuator dynamics in adaptive controller design for WMRs. In [10], the authors addressed the trajectory tracking problem for a WMR, using the extended Kalman filter to observe disturbances along nonlinear dynamics. A sliding mode control for path-tracking unmanned agricultural vehicles with adaption laws was presented in [2]. These endeavors underscore that most control techniques for WMRs rely on variable structures or adaptive mechanisms.

Takagi–Sugeno (T–S) fuzzy model-based strategy is well recognized as an efficient solution for nonlinear control systems [6, 7, 9], including WMRs. Sun et al. [15] proposed a continuous-time T–S fuzzy control design for WMR with visual odometry. This paper continues these efforts to develop a sampled-data approach for WMRs with disturbances and uncertainties using the T–S framework. The focal points of consideration are twofold: (i) disturbance attenuation and (ii) sampled-data burden.

(i) While WMRs conventionally assume pure rolling of wheels, local floor irregularities may cause a slip, which can be identified by $\mathcal{L}_2$ disturbances. The driving task of a WMR is, therefore, defined as the energy-to-peak disturbance attenuation problem in trajectory tracking. In [1], the robust energy-to-peak filtering problem for uncertain continuous-time T–S fuzzy models was studied. In [18], a continuous-time energy-to-peak output-tracking controller was developed for nonlinearly perturbed systems. However, few research efforts are found devoted to the $\mathcal{L}_2$–$\mathcal{L}_\infty$ disturbance attenuation problem for WMRs.

(ii) Given the prevalence of low-cost digital microprocessors for driving electric actuators, discrete-time model-based sampled-data control methodologies have become

✉ Ho Jae Lee
mylchi@inha.ac.kr

[1] Korea Institute of Robotics & Technology Convergence, Pohang 37666, Korea

[2] Department of Electronic Engineering, Inha University, Incheon 22212, Korea

Published online: 17 April 2024

imperative. However, deriving an exact discrete-time model for a WMR proves often unattainable due to the nonlinear nature of the initial value problem [8]. In [4], a predictive control technique was examined, where an approximate discrete-time error posture model of a WMR was used; thereby, actual performance may be degraded. Fast sampling is essential for preventing the performance degradation of sampled-data control. However, it significantly strains the network bandwidth and computing capability of the microprocessor. The event-triggered—rather than the ordinary fixed time-triggering—control (ETC), which changes the control input only when a specific event occurs, can be a resolution [3]. Previous work [11] polished an ETC scheme with a nonlinear sliding mode control technique for WMRs, validating the theoretical development through experimentation.

This paper offers a robust fuzzy sampled-data ETC approach for path tracking of uncertain nonholonomic WMRs that achieves energy-to-peak disturbance attenuation. The kinematic model of a nonlinear WMR is represented in the T–S fuzzy form with no modeling errors. The suggested scheme analyzes closed-loop stability in the continuous-time domain, hence removing the need for a discrete-time model of a WMR. The design condition is stated in terms of linear matrix inequalities and ensures the Zeno-free behavior of the event triggering. A numerical example of a WMR demonstrates the efficacy of the proposed method.

Notation: The index set is defined as $\mathcal{I}_R := \{1, \ldots, r\} \subset \mathbb{N}$. $\mathcal{I}_J \times \mathcal{I}_R$ denotes all pairs $(i, j) \in \mathcal{I}_R \times \mathcal{I}_R$ such that $1 \leqslant i < j \leqslant r$. The shorthand $\mathrm{He}\{X\} := X + X^{\mathrm{T}}$ is adopted, and the transposed element in symmetric positions is denoted by $*$.

2 Kinematics of a WMF and its T–S Fuzzy Modeling

For a mechanical kinematics with the n-dimensional generalized coordinates q, the m nonholonomic independent constraints can be expressed as:

$$A(q)\dot{q} = 0$$

where $A(q) : \mathbb{R}^n \to \mathbb{R}^{m\times n}$ is a function matrix with full row rank. For $n - m$ linear independent vector fields $s_i(q)$ that comprise the basis for the nullspace of $A(q)$, we obtain

$$A(q)\underbrace{\begin{bmatrix} s_1(q) \cdots s_{n-m}(q) \end{bmatrix}}_{=:J(q)} = 0$$
$$\implies \dot{q} \in \mathrm{span}\{s_1(q), \ldots, s_{n-m}(q)\}.$$

Then, there exists a velocity vector $p \in \mathbb{R}^{n-m}$ [13, 19] such that

$$\dot{q} = J(q)p.$$

In this study, as shown in Fig. 1, we consider a two-wheeled mobile robot whose posture is represented by the generalized coordinate $q := (x, y, \phi) \in \mathbb{R}^3$ in the world X–Y frame. In this case, (x, y) is the Cartesian coordinates of the center of mass of the vehicle, and ϕ is the counterclockwise angle between the heading direction and the X-axis.

Assumption 1 ([19]) The WMR purely rolls and does not slip in a lateral direction.

Assumption 1 poses a nonholonomic restriction in which the velocity in the lateral direction of a WMR is null, which is represented by

$$-\dot{x}\sin(\phi) + \dot{y}\cos(\phi) = 0$$
$$\iff \underbrace{\begin{bmatrix} -\sin(\phi) & \cos(\phi) & 0 \end{bmatrix}}_{A(q)}\dot{q} = 0.$$

Two vector fields, $s_1 = (\cos(\phi), \sin(\phi), 0)$ and $s_2 = (0, 0, 1)$ are linearly independent and lie in the nullspace of $A(q)$. We define $p := (v, \omega)$, where v represents the linear velocity in the heading direction and ω denotes the angular velocity. The kinematics model is constructed as

$$\underbrace{\begin{bmatrix} \dot{x} \\ \dot{y} \\ \dot{\phi} \end{bmatrix}}_{\dot{q}} = \underbrace{\begin{bmatrix} \cos(\phi) & 0 \\ \sin(\phi) & 0 \\ 0 & 1 \end{bmatrix}}_{J(q)} \underbrace{\begin{bmatrix} v \\ \omega \end{bmatrix}}_{p} \quad (1)$$

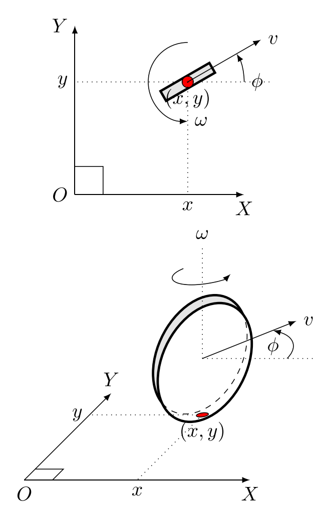

Fig. 1 The posture of WMR

The reference posture $q_r := (x_r, y_r, \phi_r)$ that the WMR is to follow is subject to

$$\begin{bmatrix} \dot{x}_r \\ \dot{y}_r \\ \dot{\phi}_r \end{bmatrix} = \begin{bmatrix} \cos(\phi_r) & 0 \\ \sin(\phi_r) & 0 \\ 0 & 1 \end{bmatrix} \begin{bmatrix} v_r \\ \omega_r \end{bmatrix} \quad (2)$$

where $(v_r, \omega_r) =: p_r$ is a reference velocity vector.

The error posture (i.e. the tracking error with respect to the frame of the WMR defined as the Cartesian coordinate system with an origin of (x, y) and X-axis in the direction of ϕ) is calculated by

$$e = \begin{bmatrix} e_x \\ e_y \\ e_\phi \end{bmatrix} := \begin{bmatrix} \cos(\phi) & \sin(\phi) & 0 \\ -\sin(\phi) & \cos(\phi) & 0 \\ 0 & 0 & 1 \end{bmatrix} (q_r - q). \quad (3)$$

Considering Eq. 1, the dynamic behavior of Eq. 3 is represented as follows:

$$\begin{bmatrix} \dot{e}_x \\ \dot{e}_y \\ \dot{e}_\phi \end{bmatrix} = \begin{bmatrix} \cos(e_\phi) & 0 \\ \sin(e_\phi) & 0 \\ 0 & 1 \end{bmatrix} \begin{bmatrix} v_r \\ \omega_r \end{bmatrix} + \begin{bmatrix} -1 & e_y \\ 0 & -e_x \\ 0 & -1 \end{bmatrix} \begin{bmatrix} v \\ \omega \end{bmatrix}.$$

We take p in the form of

$$p := \begin{bmatrix} v_r \cos(e_\phi) \\ \omega_r \end{bmatrix} + u. \quad (4)$$

Overall, the nonlinear error-posture model of a WMR is constructed as follows:

$$\dot{e} = \begin{bmatrix} 0 & \omega_r & 0 \\ -\omega_r & 0 & \frac{v_r \sin(e_\phi)}{e_\phi} \\ 0 & 0 & 0 \end{bmatrix} e + \begin{bmatrix} -1 & e_y \\ 0 & -e_x \\ 0 & -1 \end{bmatrix} u. \quad (5)$$

The four nonlinear parameters that appeared in Eq. 5 can be expressed by the following convex combinations:

$$\omega_r = \sum_{j=1}^{2} \mu_1^j a_1^j, \quad \frac{v_r \sin(e_\phi)}{e_\phi} = \sum_{j=1}^{2} \mu_2^j a_2^j$$

$$e_y = \sum_{j=1}^{2} \mu_3^j a_3^j, \quad e_x = \sum_{j=1}^{2} \mu_4^j a_4^j.$$

Using the sector nonlinearity technique [5], we solve these equations to obtain:

$$\mu_1^i = \begin{cases} \dfrac{\omega_r - a_1^2}{a_1^1 - a_1^2}, & \text{for } i = 1, \\ 1 - \mu_1^1, & \text{otherwise} \end{cases}$$

$$\mu_2^i = \begin{cases} \dfrac{\frac{v_r \sin(e_\phi)}{e_\phi} - a_2^2}{a_2^1 - a_2^2}, & \text{for } i = 1, \\ 1 - \mu_2^1, & \text{otherwise} \end{cases}$$

$$\mu_3^i = \begin{cases} \dfrac{e_y - a_3^2}{a_3^1 - a_3^2}, & \text{for } i = 1, \\ 1 - \mu_3^1, & \text{otherwise} \end{cases}$$

$$\mu_4^i = \begin{cases} \dfrac{e_x - a_4^2}{a_4^1 - a_4^2}, & \text{for } i = 1, \\ 1 - \mu_4^1, & \text{otherwise} \end{cases}$$

where a_j^i, $(i, j) \in \mathcal{I}_2 \times \mathcal{I}_4$ are determined as follows:

$$\left.\begin{aligned} a_1^1 &\geqslant \sup_{\omega_r \in [a_1^1, a_1^2]} \omega_r \\ a_1^2 &\leqslant \inf_{\omega_r \in [a_1^1, a_1^2]} \omega_r \end{aligned}\right\} \implies \mu_1^i \in \mathbb{R}_{[0,1]}$$

$$\left.\begin{aligned} a_2^1 &\geqslant \sup_{\frac{v_r \sin(e_\phi)}{e_\phi} \in [a_2^1, a_2^2]} \frac{v_r \sin(e_\phi)}{e_\phi} \\ a_2^2 &\leqslant \inf_{\frac{v_r \sin(e_\phi)}{e_\phi} \in [a_2^1, a_2^2]} \frac{v_r \sin(e_\phi)}{e_\phi} \end{aligned}\right\} \implies \mu_2^i \in \mathbb{R}_{[0,1]}$$

$$\left.\begin{aligned} a_3^1 &\geqslant \sup_{e_y \in [a_3^1, a_3^2]} e_y \\ a_3^2 &\leqslant \inf_{e_y \in [a_3^1, a_3^2]} e_y \end{aligned}\right\} \implies \mu_3^i \in \mathbb{R}_{[0,1]}$$

$$\left.\begin{aligned} a_4^1 &\geqslant \sup_{e_x \in [a_4^1, a_4^2]} e_x \\ a_4^2 &\leqslant \inf_{e_x \in [a_4^1, a_4^2]} e_x \end{aligned}\right\} \implies \mu_4^i \in \mathbb{R}_{[0,1]}.$$

We set $z := \left(\omega_r, \frac{v_r \sin(e_\phi)}{e_\phi}, e_y, e_x\right) \in \mathbb{R}^4$ as the premise variables for the T–S fuzzy model of Eq. 5. If the membership function Γ_j^i of z_j in the ith fuzzy inference rule is set as follows:

$$\Gamma_1^i = \begin{cases} \mu_1^1, & \text{for } i = \{1, \ldots, 8\} \\ \mu_1^2, & \text{otherwise} \end{cases}$$

$$\Gamma_2^i = \begin{cases} \mu_2^1, & \text{for } i = \{1,\dots,4,9,\dots,12\} \\ \mu_2^2, & \text{otherwise} \end{cases}$$
$$\Gamma_3^i = \begin{cases} \mu_3^1, & \text{for } i = \{1,2,5,6,9,10,13,14\} \\ \mu_3^2, & \text{otherwise} \end{cases}$$
$$\Gamma_4^i = \begin{cases} \mu_4^1, & \text{for } i = \{1,3,5,7,9,11,13,15\} \\ \mu_4^2, & \text{otherwise} \end{cases}$$

the following state equation

$$\dot{e} = \sum_{i=1}^{16} \theta_i (A_i e + B_i u) \tag{6}$$

is the modeling error-free T–S fuzzy model for Eq. 5 on the domain $[a_1^1, a_1^2] \times [a_2^1, a_2^2] \times [a_3^1, a_3^2] \times [a_4^1, a_4^2] \subset \mathbb{R}^4$, where

$$\theta_i(z) := \frac{\prod_{j=1}^{4} \Gamma_j^i(z_j)}{\sum_{i=1}^{16} \left(\prod_{j=1}^{4} \Gamma_j^i(z_j) \right)}$$

and

$$A_i = \begin{bmatrix} 0 & (2,1) & 0 \\ -(2,1) & 0 & (2,3) \\ 0 & 0 & 0 \end{bmatrix}, \quad B_i = \begin{bmatrix} -1 & (1,2) \\ 0 & (2,2) \\ 0 & -1 \end{bmatrix}$$

where

$$(2,1) = \begin{cases} a_1^1, & \text{for } i = \{1,\dots,8\} \\ a_1^2, & \text{otherwise} \end{cases}$$
$$(2,3) = \begin{cases} a_2^1, & \text{for } i = \{1,\dots,4,9,\dots,12\} \\ a_2^2, & \text{otherwise} \end{cases}$$
$$(1,2) = \begin{cases} a_3^1, & \text{for } i = \{1,2,5,6,9,10,13,14\} \\ a_3^2, & \text{otherwise} \end{cases}$$
$$(2,2) = \begin{cases} a_4^1, & \text{for } i = \{1,3,5,7,9,11,13,15\} \\ a_4^2, & \text{otherwise.} \end{cases}$$

3 Robust $\mathcal{L}_2$–$\mathcal{L}_\infty$ ETC Design

To strengthen the robustness to uncertainties and disturbances attenuation performance in design, we modify (6) as follows:

$$\begin{cases} \dot{e} = \sum_{i=1}^{r} \theta_i ((A_i + \Delta A_i)e + B_i u + B_{w_i} w) \\ z = \sum_{i=1}^{r} \theta_i C_{z_i} e \end{cases} \tag{7}$$

where ΔA_i denotes the system uncertainty and $z \in \mathbb{R}$ is the performance output.

With a slight abuse of notation, the Lebesgue space $\mathcal{L}_p^n[0,\infty)$ of measurable functions $f : [0,\infty) \to \mathbb{R}^n$ satisfies

$$\|f\|_{\mathcal{L}_{p,r}^n} := \begin{cases} \left(\int_0^\infty \|f(t)\|_r^p \, \mathrm{d}t \right)^{1/p} < \infty & \text{for} 1 \leqslant p < \infty \\ \sup_{t \in \mathbb{R}_{\geqslant 0}} \|f(t)\|_r < \infty & \text{for} p = \infty \end{cases}$$

where the following conventional vector r-norm is adopted [12]:

$$\|f\|_r := \begin{cases} \left(\sum_{i=1}^{n} |f_i(t)|^r \right)^{1/r} < \infty & \text{for} 1 \leqslant r < \infty \\ \max_{i \in \mathcal{I}_R} |f_i(t)| < \infty & \text{for} r = \infty. \end{cases}$$

In this study, we consider a continuous-time disturbance $w \in \mathcal{L}_{2,2}^p$ and a continuous-time performance output $z \in \mathcal{L}_{\infty,2}^q$ (simply denoted as $\mathcal{L}_2$ and $\mathcal{L}_\infty$, respectively). In addition, their norms $\|w\|_{\mathcal{L}_{2,2}^p}$ and $\|z\|_{\mathcal{L}_{\infty,2}^q}$ are denoted by $\|w\|_2$ and $\|z\|_\infty$, respectively.

Assumption 2 There exist known compatible constant matrices D and E and an unknown time-varying diagonal matrix Δ satisfying $\Delta^{\mathrm{T}}\Delta \preccurlyeq I, \forall t \in \mathbb{R}_{\geqslant 0}$ such that

$$\Delta A = D \Delta E.$$

Lemma 1 ([17]) *Given compatible matrices D, E, $S = S^{\mathrm{T}}$, with $\Delta \ni \Delta^{\mathrm{T}}\Delta \preccurlyeq I$, there exists $\epsilon \in \mathbb{R}_{>0}$ such that*

$$S + \mathrm{He}\{D\Delta E\} \prec 0$$
$$\iff S + \begin{bmatrix} D & E^{\mathrm{T}} \end{bmatrix} \begin{bmatrix} \epsilon^{-1} I & * \\ 0 & \epsilon I \end{bmatrix} \begin{bmatrix} D^{\mathrm{T}} \\ E \end{bmatrix} \prec 0.$$

Lemma 2 ([9]) *Given compatible matrices D, $Q = Q^{\mathrm{T}} \succ 0$, $S = S^{\mathrm{T}}$, the following equivalence is true:*

$$S + D^{\mathrm{T}} Q D \prec 0 \iff \begin{bmatrix} S & * \\ D & -Q^{-1} \end{bmatrix} \prec 0.$$

We employ the following event-triggered aperiodic sampled-data controller:

$$u = u_k := \sum_{i=1}^{r} \theta_{i_k} K_i e(t_k), \quad t \in [t_k, t_{k+1}) \tag{8}$$

where t_k, $k \in \mathbb{Z}_{\geqslant 0}$ represents the time at which the control input is updated and $\theta_{i_k} := \theta_i(z(t_k))$. The subsequent execution time t_{k+1} is determined by the following event-triggering mechanism:

$$t_{k+1} := \inf \Bigg\{ t \in \mathbb{R}_{\geqslant 0} : t > t_k \wedge \sigma e^{\mathrm{T}} P e \leqslant 2 e^{\mathrm{T}} \Bigg(\sum_{i,j=1}^{r} \theta_i \theta_{j_k} P B_i K_j \Bigg) \epsilon_e \Bigg\} \tag{9}$$

where $\epsilon_e := e(t_k) - e$, $\sigma \in \mathbb{R}_{>0}$ is a given threshold, and P is a positive definite matrix.

The problem of interest is expressed as follows:

Problem 1 *Find K_i such that the uncertain fuzzy model (7) closed by the aperiodic sampled-data controller (8) updated by the event-triggering mechanism (9) exhibits the following $\mathcal{L}_2$–$\mathcal{L}_\infty$ disturbance attenuation performance*

$$\|z\|_\infty \leqslant e^{\mathrm{T}}(0) P e(0) + \gamma \|w\|_2 \tag{10}$$

and is robustly asymptotically stable against the norm-bounded parametric uncertainties when $w = 0$.

The close-loop system of Eqs. 7, 8, and 9 is constructed as

$$\dot{e} = \sum_{i=1}^{r} \theta_i \theta_{j_k} ((A_i + \Delta A_i + B_i K_j) e + B_i K_j \epsilon_e + B_{w_i} w) \tag{11}$$

for $t \in [t_k, t_{k+1})$. Similar to [20], we introduce the following relation about the asynchronous firing strengths

$$\theta_{i_k} = \rho_i^k \theta_i, \quad t \in [t_k, t_{k+1})$$

and suppose the existence of $\underline{\rho}, \overline{\rho} \in \mathbb{R}_{>0}$ such that

$$\underline{\rho} := \min_{(i,k) \in \mathcal{I}_R \times \mathbb{Z}_{\geqslant 0}} \rho_i^k, \quad \overline{\rho} := \max_{(i,k) \in \mathcal{I}_R \times \mathbb{Z}_{\geqslant 0}} \rho_i^k. \tag{12}$$

Then, it straightforwardly follows that

$$\frac{\underline{\rho}}{\overline{\rho}} \leqslant \frac{\rho_i^k}{\rho_j^k} \leqslant \frac{\overline{\rho}}{\underline{\rho}}.$$

The following theorem proposes a design condition for Problem 1.

Theorem 1 *Given γ, κ_i, λ, σ, $\underline{\rho}$, and $\overline{\rho}$, the uncertain fuzzy model (7) closed by the aperiodic sampled-data controller (8) updated by the event-triggering mechanism (9) (i) exhibits the γ-$\mathcal{L}_2$–$\mathcal{L}_\infty$ disturbance attenuation performance (10) and (ii) is implementable if there exist M_i, $Q = Q^{\mathrm{T}} \succ 0$ such that*

$$\Xi_{ii} \prec 0, \quad i \in \mathcal{I}_R \tag{13}$$

$$\Xi_{ij} + \frac{\underline{\rho}}{\overline{\rho}} \Xi_{ji} \prec 0 \tag{14}$$

$$\Xi_{ij} + \frac{\overline{\rho}}{\underline{\rho}} \Xi_{ji} \prec 0, \quad (i,j) \in \mathcal{I}_J \times \mathcal{I}_R \tag{15}$$

$$\begin{bmatrix} Q & * \\ C_{z_i} Q & I \end{bmatrix} \succ 0, \quad i \in \mathcal{I}_R \tag{16}$$

where

$$\Xi_{ij} := \begin{bmatrix} \begin{pmatrix} \mathrm{He}\{A_i Q + B_i M_j\} \\ +(\lambda + \sigma) Q \end{pmatrix} & * & * & * \\ B_{w_i}^{\mathrm{T}} & -\gamma^2 I & * & * \\ D_i^{\mathrm{T}} & 0 & -\kappa_i I & * \\ E_i Q & 0 & 0 & -\kappa_i^{-1} I \end{bmatrix}.$$

In this case, the gain is given by $K_i = M_i Q^{-1}$.

Proof (i) To prove stability, we define $V := e^{\mathrm{T}} P e$ with $P = P^{\mathrm{T}} \succ 0$. The time derivative of V is computed as

$$\dot{V} = e^{\mathrm{T}} \left(\mathrm{He} \left\{ \sum_{i,j=1}^{r} \theta_i \theta_{j_k} P (A_i + \Delta A_i + B_i K_j) \right\} \right) e + 2 e^{\mathrm{T}} \left(\sum_{i,j=1}^{r} \theta_i \theta_{j_k} P B_i K_j \right) \epsilon_e + 2 e^{\mathrm{T}} \left(\sum_{i=1}^{r} \theta_i P B_{w_i} \right) w$$

for $t \in [t_k, t_{k+1})$. Using Eq. 9, we can majorize

$$\begin{aligned} \dot{V} &\leqslant e^{\mathrm{T}} \left(\mathrm{He} \left\{ \sum_{i,j=1}^{r} \theta_i \theta_{j_k} P (A_i + \Delta A_i + B_i K_j) \right\} \right) e \\ &\quad + \sigma e^{\mathrm{T}} P \epsilon_{\mathrm{e}} + 2 e^{\mathrm{T}} \left(\sum_{i=1}^{r} \theta_i P B_{w_i} \right) w \\ &= \begin{bmatrix} e \\ w \end{bmatrix}^{\mathrm{T}} \left(\sum_{i,j=1}^{r} \theta_i \theta_{j_k} \bar{\Xi}_{ij} \right) \begin{bmatrix} e \\ w \end{bmatrix} - \lambda V + \gamma^2 w^{\mathrm{T}} w \end{aligned}$$

$$= \begin{bmatrix} e \\ w \end{bmatrix}^{\mathrm{T}} \left(\sum_{i=1}^{r} \theta_i \theta_i \rho_i^k \bar{\Xi}_{ii} + \sum_{i<j}^{r} \theta_i \theta_j \left(\rho_j^k \bar{\Xi}_{ij} + \rho_i^k \bar{\Xi}_{ji} \right) \right)$$
$$\times \begin{bmatrix} e \\ w \end{bmatrix} - \lambda V + \gamma^2 w^{\mathrm{T}} w$$
$$= \begin{bmatrix} e \\ w \end{bmatrix}^{\mathrm{T}} \left(\sum_{i=1}^{r} \theta_i \theta_i \rho_i^k \bar{\Xi}_{ii} + \sum_{i<j}^{r} \theta_i \theta_j \rho_j^k \left(\bar{\Xi}_{ij} + \frac{\rho_i^k}{\rho_j^k} \bar{\Xi}_{ji} \right) \right)$$
$$\times \begin{bmatrix} e \\ w \end{bmatrix} - \lambda V + \gamma^2 w^{\mathrm{T}} w$$

where

$$\bar{\Xi}_{ij} := \begin{bmatrix} \mathrm{He}\left\{ P(A_i + \Delta A_i + B_i K_j) \right\} + (\sigma + \lambda) P & * \\ B_{w_i}^{\mathrm{T}} P & -\gamma^2 I \end{bmatrix}.$$

Define

$$\eta_1 := \frac{\frac{\overline{\rho}}{\underline{\rho}} - \frac{\rho_i^k}{\rho_j^k}}{\frac{\overline{\rho}}{\underline{\rho}} - \frac{\underline{\underline{\rho}}}{\overline{\overline{\rho}}}}, \quad \eta_2 := \frac{\frac{\rho_i^k}{\rho_j^k} - \frac{\underline{\underline{\rho}}}{\overline{\overline{\rho}}}}{\frac{\overline{\rho}}{\underline{\rho}} - \frac{\underline{\underline{\rho}}}{\overline{\overline{\rho}}}}$$

where one knows that $\eta_1, \eta_2 \in \mathbb{R}_{[0,1]}$ and $\eta_1 + \eta_2 = 1$. Applying a similarity transformation with $\mathrm{diag}(Q^{-1}, I, I, I)$, Lemmas 1 and 2, and Assumption 2 to Eqs. 14 and 15 and denoting $Q^{-1} = P$ and $M_i = K_i Q$ results in

$$\eta_1 \left(\bar{\Xi}_{ij} + \frac{\underline{\underline{\rho}}}{\overline{\overline{\rho}}} \bar{\Xi}_{ji} \right) + \eta_2 \left(\bar{\Xi}_{ij} + \frac{\overline{\rho}}{\underline{\rho}} \bar{\Xi}_{ji} \right) \prec 0$$
$$\Longrightarrow \bar{\Xi}_{ij} + \frac{\rho_i^k}{\rho_j^k} \bar{\Xi}_{ji} \prec 0.$$

Similarly, it holds that Eq. 13 $\Longrightarrow$ $\bar{\Xi}_{ii} \prec 0$. As a result

$$\dot{V} < -\lambda V + \gamma^2 w^{\mathrm{T}} w. \tag{17}$$

By the comparison lemma, we know that

$$V < V(0) + \gamma^2 \int_0^\infty w^{\mathrm{T}} w \, \mathrm{d}\tau.$$

Next, performing a similarity transformation with $\mathrm{diag}(P^{-1}, I)$ and applying Lemma 2 to Eq. 16, we derive

$$(16) \iff P - \left(\sum_i^r \theta_i C_{z_i} \right)^{\mathrm{T}} \left(\sum_i^r \theta_i C_{z_i} \right) \succ 0$$
$$\iff V - z^{\mathrm{T}} z > 0, \quad \forall t \in \mathbb{R}_{\geqslant 0}.$$

Then, we arrive at

$$\|z\|_\infty = \sup_{t \in \mathbb{R}_{\geqslant 0}} \|z\| < \sqrt{V(0) + \gamma^2 \int_0^\infty w^{\mathrm{T}} w \, \mathrm{d}\tau}$$
$$\leqslant \sqrt{e^{\mathrm{T}}(0) P e(0)} + \gamma \|w\|_2 .$$

When $w = 0, \forall t \in \mathbb{R}_{>0}$, Eq. 17 can be expressed as $\dot{V} + \lambda V < 0 \implies \dot{V} < 0$. Therefore, Eq. 11 is robustly asymptotically stable.

(ii) To demonstrate the implementability of Eq. 8, we investigate the existence of a nonzero lower bound of the minimum event-triggering interval in Eq. 9. Because $e(t_k)$ is a constant for any interval $[t_k, t_{k+1})$, we construct

$$\dot{\epsilon}_e = \dot{e}(t_k) - \dot{e}$$
$$= 0 - \left(\sum_{i=1}^{r} \theta_i \theta_{j_k} ((A_i + \Delta A_i) e + B_i K_j e(t_k) + B_{w_i} w) \right)$$
$$= \sum_{i=1}^{r} \theta_i \theta_{j_k} ((A_i + \Delta A_i) \epsilon_e - (A_i + \Delta A_i + B_i K_j) e(t_k)$$
$$- B_{w_i} w)$$

and we derive the following differential inequality:

$$\frac{\mathrm{d}\|\epsilon_e\|}{\mathrm{d}t} = \frac{\mathrm{d}\left(\sqrt{\epsilon_e^{\mathrm{T}} \epsilon_e}\right)}{\mathrm{d}t} = \frac{\epsilon_e^{\mathrm{T}} \dot{\epsilon}_e}{\|\epsilon_e\|}$$
$$\leqslant \left\| \frac{\mathrm{d}\epsilon_e}{\mathrm{d}t} \right\|$$
$$= \left\| \sum_{i=1}^{r} \theta_i \theta_{j_k} ((A_i + \Delta A_i) \epsilon_e \right.$$
$$\left. - (A_i + \Delta A_i + B_i K_j) e(t_k) - B_{w_i} w) \right\|$$
$$\leqslant \sum_{i=1}^{r} \theta_i \theta_{j_k} \|A_i + \Delta A_i\| \|\epsilon_e\|$$
$$+ \sum_{i=1}^{r} \theta_i \theta_{j_k} \left\| (A_i + \Delta A_i + B_i K_j) \right\| \|e(t_k)\|$$
$$+ \sum_{i=1}^{r} \theta_i \theta_{j_k} \left\| B_{w_i} \right\| \|w\|$$
$$\leqslant c_1 \|\epsilon_e\| + c_2 \|e\| + c_3 \|w\|$$

where

$$c_1 := \max_{i \in \mathcal{I}_R} (\|A_i\| + \|D_i\| \|E_i\|)$$
$$c_2 := \max_{(i,j) \in \mathcal{I}_R \times \mathcal{I}_R} \left(\|A_i\| + \|D_i\| \|E_i\| + \left\| B_i K_j \right\| \right)$$
$$c_3 := \max_{i \in \mathcal{I}_R} \left\| B_{w_i} \right\| .$$

Because of $\epsilon_e(t_k) = 0$, the comparison lemma yields

$$\|\epsilon_e\| \leqslant \frac{1}{c_1}\left(c_2\|e\| + c_3\|w\|\right)\left(e^{c_1(t-t_k)} - 1\right).$$

Solving the inequality, we obtain

$$\begin{aligned} t_{k+1} &> t_k + \frac{1}{c_1}\ln\left(1 + \frac{c_1\|\epsilon_e\|}{c_2\|e\| + c_3\|w\|}\right) \\ &> t_k + \frac{1}{c_1}\ln\left(1 + \frac{c_1\|P\|\,\|e\|}{c_2\|e\| + c_3\|w\|}\right) \end{aligned}$$

where c_1, c_2, c_3 are positively finite. Therefore, for any $k \in \mathbb{Z}_{\geqslant 0}$, $t_{k+1} - t_k > 0$. This completes the proof. □

4 A Numerical Example

The parameters for Eq. 6 are set as follows:

$$\begin{aligned} &a_1^1 = 0.7, \quad a_1^2 = 2.1, \quad a_2^1 = 1.7, \quad a_2^2 = 5.1 \\ &a_3^1 = -0.2, \quad a_3^2 = 0.2, \quad a_4^1 = -0.2, \quad a_4^2 = 0.2. \end{aligned}$$

In addition, we introduce the following uncertainty, the disturbance, and the controlled output for Eq. 7, parameterized as

$$\Delta A_i = \begin{bmatrix} 0 & 0 & 0 \\ 0.09\delta & 0 & 0 \\ 0 & 0 & 0 \end{bmatrix}, \quad B_{w_i} = \begin{bmatrix} 0.1 \\ 0.1 \\ 0.1 \end{bmatrix}$$
$$C_{z_i} = \begin{bmatrix} 0.1 & 0.1 & 0.1 \end{bmatrix}$$

where $\delta \ni |\delta| \leqslant 1$ randomly varies over time. According to Assumption 2, ΔA_i is decomposed as

$$D_i = \begin{bmatrix} 0 \\ 0.3 \\ 0 \end{bmatrix}, \quad \Delta_i = \delta, \quad E_i = \begin{bmatrix} 0.03 & 0 & 0 \end{bmatrix}.$$

For Problem 1, the following $\mathcal{L}_2$ disturbance

$$w = \begin{cases} 0.2\sin(5t), & \text{for } 0.5 \leqslant t \leqslant 2.5 \\ 0, & \text{otherwise} \end{cases}$$

is considered.

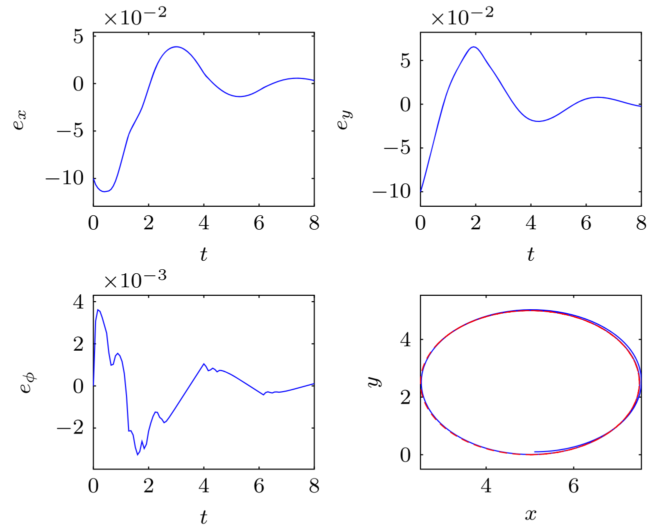

Fig. 2 Time responses of the closed-loop error posture of the WMR

Let $\gamma = 0.5$, $\kappa_i = 0.1$, $\lambda = 0.05$, $\sigma = 0.05$, $\underline{\rho} = 0.4$, and $\overline{\rho} = 2$. The following controller gains are obtained through Theorem 1

$$K_1 = \begin{bmatrix} 0.3504 & -0.3492 & -8.3397 \\ 0.0213 & 0.3603 & 9.0552 \end{bmatrix}$$
$$K_2 = \begin{bmatrix} 0.3667 & -0.4126 & -10.3738 \\ 0.0491 & 0.4022 & 9.5734 \end{bmatrix}$$
$$K_3 = \begin{bmatrix} 0.3741 & -0.3005 & -7.0670 \\ 0.0248 & 0.3988 & 10.1102 \end{bmatrix}$$
$$K_4 = \begin{bmatrix} 0.3729 & -0.2095 & -5.1207 \\ -0.0117 & 0.4600 & 10.7983 \end{bmatrix}$$
$$K_5 = \begin{bmatrix} 0.3929 & -0.4072 & -9.7786 \\ 0.0286 & 0.4743 & 11.4819 \end{bmatrix}$$

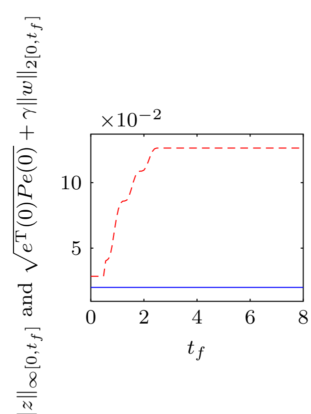

Fig. 3 Energy-to-peak disturbance attenuation performance: $\sqrt{e^{\mathrm{T}}(0)Pe(0)} + \gamma\|w\|_2$ (dashed (red)) and $\|z\|_\infty$ (solid (blue))

$$K_6 = \begin{bmatrix} 0.4193 & -0.5125 & -12.9243 \\ 0.0735 & 0.5254 & 12.4182 \end{bmatrix}$$

$$K_7 = \begin{bmatrix} 0.4241 & -0.3340 & -7.8688 \\ 0.0239 & 0.5425 & 13.3227 \end{bmatrix}$$

$$K_8 = \begin{bmatrix} 0.4232 & -0.1951 & -4.6053 \\ -0.0333 & 0.6183 & 14.5886 \end{bmatrix}$$

$$K_9 = \begin{bmatrix} 0.5294 & -0.5946 & -14.2628 \\ 0.0564 & 0.6087 & 15.7089 \end{bmatrix}$$

$$K_{10} = \begin{bmatrix} 0.5808 & -0.7989 & -20.0466 \\ 0.1388 & 0.6732 & 17.1337 \end{bmatrix}$$

$$K_{11} = \begin{bmatrix} 0.5989 & -0.5320 & -12.5214 \\ 0.0629 & 0.7208 & 18.7482 \end{bmatrix}$$

$$K_{12} = \begin{bmatrix} 0.6021 & -0.2888 & -6.6145 \\ -0.0411 & 0.8237 & 20.6653 \end{bmatrix}$$

$$K_{13} = \begin{bmatrix} 0.6701 & -0.7829 & -18.9559 \\ 0.0874 & 0.9009 & 22.9529 \end{bmatrix}$$

$$K_{14} = \begin{bmatrix} 0.7650 & -1.1476 & -28.9424 \\ 0.2326 & 1.0011 & 25.6495 \end{bmatrix}$$

$$K_{15} = \begin{bmatrix} 0.7873 & -0.6738 & -15.9035 \\ 0.0731 & 1.1158 & 28.6405 \end{bmatrix}$$

$$K_{16} = \begin{bmatrix} 0.8039 & -0.2641 & -5.4255 \\ -0.1122 & 1.3003 & 32.7024 \end{bmatrix}.$$

(i) Reference velocities are set as

$$\begin{bmatrix} v_r \\ \omega_r \end{bmatrix} = \begin{bmatrix} 5(1 - 0.5e^{-0.1t}) \\ 2(1 - 0.5e^{-0.1t}) \end{bmatrix}$$

to generate the reference trajectory (dash-red) for Eq. 2 with $q_r(0) = (5, 0, 0)$ shown in the lower-right subfigure of Fig. 2.

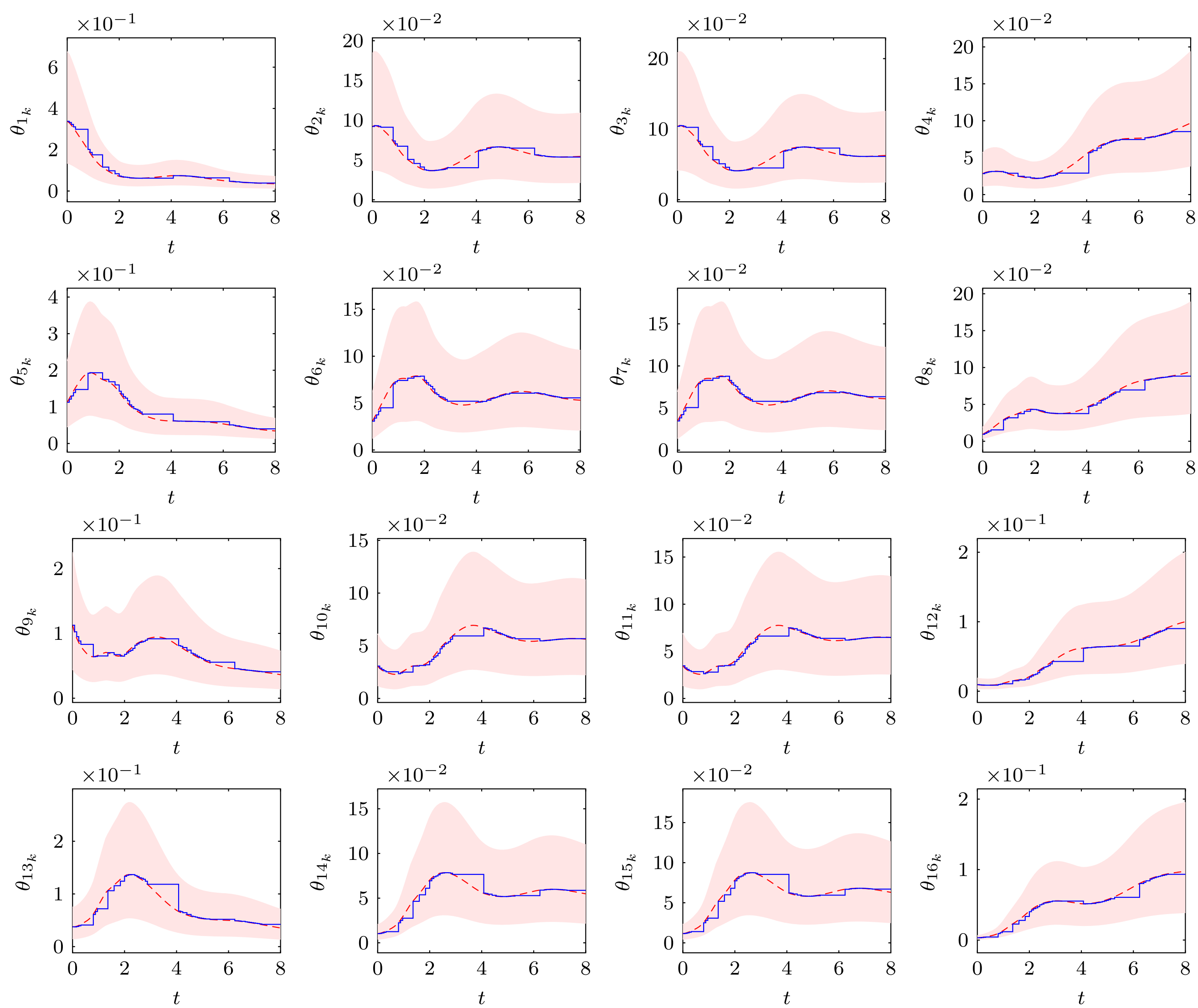

Fig. 4 Time responses of firing strengths: θ_i (dashed-red), $[\underline{\rho}\theta_i, \overline{\rho}\theta_i]$ (filled-light red), θ_{k_i} (solid-blue)

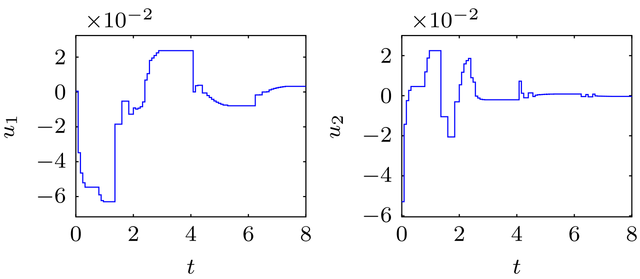

Fig. 5 Event-triggered aperiodic sampled-data control inputs

It is also shown that the controlled trajectory (solid-blue) with $q(0) = (5.1.0.1, 0)$ is accurately directed to the reference trajectory. The other subfigures in Fig. 2 depict the closed-loop time responses of Eqs. 5, 8, 9, where all the error posture variables are well bounded in the presence of the $\mathcal{L}_2$ disturbance and parametric uncertainties. As shown in Fig. 3, $\|z\|_\infty$ is smaller than $\sqrt{e^{\mathrm{T}}(0)Pe(0)}+\gamma\ \|w\|_2$ for all $t_f \in \mathbb{R}_{\geqslant 0}$, implying the proposed controller satisfies the $\mathcal{L}_2$–$\mathcal{L}_\infty$ disturbance attenuation performance in Eq. 10 over the entire simulation time horizon. It is visible from Fig. 4 that every θ_{i_k} (solid-blue) is present between the interval $[\underline{\rho}\theta_i, \overline{\rho}\theta_i]$ (filled-light red). Hence, Eq. 12 holds.

(ii) Figure 5 illustrates the ETC inputs for Eq. 8, where the control inputs are piecewise-constant but their time intervals are uneven. Figure 6 depicts the event-triggering interval versus the event-triggering instant. The discrete-time signal does not converge to zero, indicating that the proposed controller operates well in a sampled-data manner without the Zeno behavior affecting the sampling process. Thus, the proposed controller is implementable. In summary, Problem 1 is solved.

5 Conclusions

Leveraging the T–S fuzzy technique, this paper tackled the sampled-data nonlinear tracking control problem in WMRs. It is stressed that (i) the energy-to-peak disturbance attenuation was taken into consideration; and (ii) the ETC technique was adopted to overcome the unavailability of the exact discrete-time model of a WMR dynamics. The numerical example demonstrated the efficacy of the proposed method, highlighting its potential to enhance the performance of autonomous agricultural vehicles and contributing valuable insights to the field of agroforestry automation.

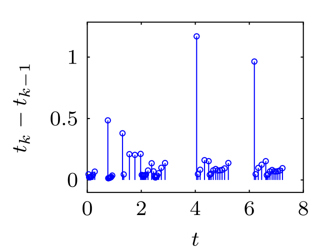

Fig. 6 Event-triggering instants and intervals

Acknowledgements This work was supported by Inha University Research Grant.

Declarations

Conflict of interest On behalf of all authors, the corresponding author states that there is no conflict of interest.

References

1. Chang XH, Park JH, Shi P (2017) Fuzzy resilient energy-to-peak filtering for continuous-time nonlinear systems. IEEE Trans Fuzzy Syst 25(6):1576–1588. https://doi.org/10.1109/tfuzz.2016.2612302
2. Ge Z, Man Z, Wang Z, Bai X, Wang X, Xiong F, Li D (2023) Robust adaptive sliding mode control for path tracking of unmanned agricultural vehicles. Comput Electr Eng 108(108):693. https://doi.org/10.1016/j.compeleceng.2023.108693
3. Jee SC, Lee HJ (2023) Positive sampled-data disturbance attenuation: separate design. Journal of Electrical Engineering & Technology. https://doi.org/10.1007/s42835-023-01637-2
4. Klančar G, Škrjanc I (2007) Tracking-error model-based predictive control for mobile robots in real time. Robot Auton Syst 55(6):460–469. https://doi.org/10.1016/j.robot.2007.01.002
5. Lee HJ (2022) Robust static output-feedback vaccination policy design for an uncertain SIR epidemic model with disturbances: positive Takagi-Sugeno model approach. Biomed Signal Process Control 72(Part A):103,273. https://doi.org/10.1016/j.bspc.2021.103273
6. Lee HJ (2023) Positivity and separation principle for observer-based output-feedback disturbance attenuation of uncertain discrete-time fuzzy models with immeasurable premise variables. J Franklin Inst 360(12):8486–8505. https://doi.org/10.1016/j.jfranklin.2023.03.047
7. Lee HJ (2023) Robust observer-based output-feedback control for epidemic models: positive fuzzy model and separation principle approach. Appl Soft Comput 132:109,802. https://doi.org/10.1016/j.asoc.2022.109802
8. Lee HJ, Kim DW (2016) Performance-recoverable intelligent digital redesign for fuzzy tracking controllers. Inf Sci 326:350–367. https://doi.org/10.1016/j.ins.2015.08.003
9. Lee HJ, Park JB, Chen G (2001) Robust fuzzy control of nonlinear systems with parametric uncertainties. IEEE Trans Fuzzy Syst 9(2):369–379. https://doi.org/10.1109/91.919258
10. Li L, Wang T, Xia Y, Zhou N (2020) Trajectory tracking control for wheeled mobile robots based on nonlinear disturbance observer with extended Kalman filter. J Franklin Inst 357(13):8491–8507. https://doi.org/10.1016/j.jfranklin.2020.04.043
11. Nath K, Yesmin A, Nanda A, Bera MK (2021) Event-triggered sliding-mode control of two wheeled mobile robot: an experimental validation. IEEE J Emerg Sel Top in Industrial Electronics 2(3):218–226. https://doi.org/10.1109/jestie.2021.3087965
12. Palhares RM, Peres PL (2000) Robust filtering with guaranteed energy-to-peak performance—an $\mathscr{LMI}$ approach. Automatica 36(6):851–858. https://doi.org/10.1016/S0005-1098(99)00211-3

13. Park BS, Yoo SJ, Park JB, Choi YH (2009) Adaptive neural sliding mode control of nonholonomic wheeled mobile robots with model uncertainty. IEEE Trans Control Syst Technol 17(1):207–214. https://doi.org/10.1109/TCST.2008.922584
14. Park BS, Yoo SJ, Park JB, Choi YH (2010) A simple adaptive control approach for trajectory tracking of electrically driven nonholonomic mobile robots. IEEE Trans Control Syst Technol 18(5):1199–1206. https://doi.org/10.1109/tcst.2009.2034639
15. Sun CH, Chen YJ, Wang YT, Huang SK (2017) Sequentially switched fuzzy-model-based control for wheeled mobile robot with visual odometry. Appl Math Model 47:765–776. https://doi.org/10.1016/j.apm.2016.11.001
16. Wang Q, He J, Lu C, Wang C, Lin H, Yang H, Li H (2023) Wu Z (2023) Modelling and control methods in path tracking control for autonomous agricultural vehicles: a review of state of the art and challenges. Appl Sci 13(12):7155. https://doi.org/10.3390/app13127155
17. Xie L (1996) Output feedback H_∞ control of systems with parameter uncertainties. Int J Control 63(4):741–750. https://doi.org/10.1080/00207179608921866
18. Xie X, Lam J, Fan C, Wang X, Kwok KW (2022) Energy-to-peak output tracking control of actuator saturated periodic piecewise time-varying systems with nonlinear perturbations. IEEE Trans Syst Man Cybern: Systems 52(4):2578–2590. https://doi.org/10.1109/tsmc.2021.3049524
19. Yang JM, Kim JH (1999) Sliding mode control for trajectory tracking of nonholonomic wheeled mobile robots. IEEE Trans Robot Autom 15(3):578–587. https://doi.org/10.1109/70.768190
20. Zhang J, Peng C (2015) Event-triggered H_∞ filtering for networked Takagi–Sugeno fuzzy systems with asynchronous constraints. IET Signal Proc 9(5):403–411. https://doi.org/10.1049/iet-spr.2014.0319
21. Zhu Z, Chen J, Yoshida T, Torisu R, Song Z, Mao E (2007) Path tracking control of autonomous agricultural mobile robots. Journal of Zhejiang University-SCIENCE A 8(10):1596–1603. https://doi.org/10.1631/jzus.2007.A1596

Sung Chul Jee received his B.S., M.S., and Ph.D. degrees from the Department of Electronic Engineering, Inha University, Incheon, Korea, in 2009, 2011, and 2014, respectively. Since 2014, he has been with Korea Institute of Robotics & Technology Convergence (KIRO), where he is currently a Principal Researcher. His research interests are robotics, automation, and fault detection.

Ho Jae Lee received his B.S., M.S., and Ph.D. degrees from the Department of Electrical and Electronic Engineering, Yonsei University, Seoul, Korea, in 1998, 2000, and 2004, respectively. In 2005, he was a Visiting Assistant Professor with the Department of Electrical and Computer Engineering, University of Houston, Houston, TX. Since 2006, he has been with the Department of Electronic Engineering, Inha University, Incheon, Korea, where he is currently a Professor. His research interests include fuzzy control systems, sampled-data control, large-scale systems, multi-agent systems, and underwater gliders.